34th Annual International Conference of the IEEE EMBS
San Diego, California USA, 28 August - 1 September, 2012

Muscle Artifact Suppression Using Independent-Component Analysis and State-Space Modeling*

Alina Santillán-Guzmán[1], Ulrich Heute[1], Ulrich Stephani[2] and Andreas Galka[2]

Abstract— **In this paper, we aim at suppressing the muscle artifacts present in electroencephalographic (EEG) signals with a technique based on a combination of Independent Component Analysis (ICA) and State-Space Modeling (SSM). The novel algorithm uses ICA to provide an initial model for SSM which is further optimized by the maximimum-likelihood approach. This model is fitted to artifact-free data. Then it is applied to data with muscle artifacts. The state space is augmented by extracting additional components from the data prediction errors. The muscle artifacts are well separated in the additional components and, hence, a suppression of them can be performed. The proposed algorithm is demonstrated by application to a clinical epilepsy EEG data set.**

I. INTRODUCTION

Electroencephalographic (EEG) recordings are widely used in neuroscience in the diagnosis and source localization of many neural disorders and phenomena, such as coma, epilepsy, and tremors [1]. The measured EEG signals are frequently contaminated with artifacts of physiological or technical origin. In the case of EEG recordings from epilepsy patients, muscle artifacts are commonly present and contaminate the signals obscuring the desired information; therefore, an efficient filtering technique is necessary. Low-Pass-Filters have been employed as a straightforward solution to suppress muscle artifacts. However, since the frequency spectrum of the brain activity and that of the muscle artifacts might overlap [2], not only the artifacts may be removed but also valuable information; an example of this are the High Frequency Oscillations (HFO) in epilepsy, whose frequency band is from 100 Hz to 1000 Hz.

In [2], Canonical-Correlation Analysis (CCA) as a Blind-Source Separation (BSS) technique (referred as BSS-CCA) is used to remove the muscle artifacts from the EEG signals. BSS-CCA tries to find sources that are uncorrelated with each other, but maximally autocorrelated. This method shows a successful removal of muscle artifacts in ictal recordings, preserving also the useful information. However, this method fails for highly non-stationary muscle artifacts. In such case, the brain activity and the artifacts are not well-separated.

Independent-Component Analysis (ICA) is also employed to separate multi-channel signals into components. Most ICA algorithms are based on two assumptions: the components must be non-Gaussian (at most one Gaussian component is allowed), and they are considered as independent. ICA has been proved as a useful technique to provide a good separation of the signals; however, it also has some weaknesses: first, the number of components is equal to or lower than the number of electrode signals; second, most of the ICA algorithms are instantaneous, i.e., they do not consider the dynamical behavior of the components [3]; third, observation noise is assumed to be absent. In [4], ICA has been applied to remove muscle artifacts in recordings from patients with Temporal-Lobe Epilepsy. However, the muscle artifacts were observed in nearly all the components and they were mixed with some brain activity. This happens because the muscle artifacts arise from many sources and, hence, the assumption of ICA of having the same number of components as channels is violated. If all the components containing the artifacts are to be suppressed, then valuable information could also be lost.

State-Space Modeling (SSM) is a technique that does not suffer from the weaknesses of ICA. However, ICA is better than SSM in detecting non-Gaussian sources, and its computational time consumption is usually lower. A connection between ICA and SSM has previously been treated in [5], where the strong aspects of both ICA and SSM have been combined and the constraint of ICA of having as many components as electrodes has been overcome.

The purpose of the work described in this paper is to suppress muscle artifacts from EEG data based on the combination of ICA and SSM described in [5].

The structure of the paper is as follows: In section II the description of the combined algorithm to suppress the muscle artifacts is explained. Section III provides the results of the application of the algorithm to real EEG data from an epilepsy patient. Conclusions are given in section IV.

II. ALGORITHM DESCRIPTION

The algorithm used in this work consists of two parts:

A. Creation of dynamical templates for brain activity, without artifacts. These templates are a model of the artifacts-free signals, and are used in the next step in the suppression of the muscle artifacts.

B. Augmentation of the brain activity dynamical templates by muscle artifactual components, to suppress the artifacts.

A. Independent-Component Analysis (ICA) and State-Space Modeling (SSM)

As a first step, it is necessary to select a data segment containing brain activity only (artifacts are not allowed).

*This work was supported by the German Research Foundation (Deutsche Forschungsgemeinschaft, DFG) through the Collaborative Research Center SFB 855 "Biomagnetic Sensing"

[1]A. Santillán-Guzmán and U. Heute are with Faculty of Engineering, Christian-Albrechts-University of Kiel, 24143 Kiel, Germany. {asg,uh} at tf.uni-kiel.de

[2]U. Stephani and A. Galka are with the Department of Neuropediatrics, Christian-Albrechts-University of Kiel, 24098 Kiel, Germany. {stephani,a.galka} at pedneuro.uni-kiel.de

An Independent-Component State-Space Model (IC-SSM) as described in [5] is employed in this work in order to suppress the muscle artifacts from brain activity.

Recalling from [6], the ICA model is given by

$$\mathbf{y}(k) = \sum_{l=1}^{m} \mathbf{c}_l s_l(k) = \mathbf{C}\mathbf{s}(k), \tag{1}$$

where $\mathbf{y}(k) = [y_1(k), ..., y_n(k)]^T$ is the mixed signal vector, k is the time instant and n denotes the number of EEG electrodes. The source signals denoted as $\mathbf{s}(k) = [s_1(k), ..., s_m(k)]^T$ are supposed to be non-Gaussian and independent. $\mathbf{C} = [\mathbf{c}_1, ..., \mathbf{c}_m]$ is an $n \times m$ mixing matrix of full rank, with $n \geq m$, i.e., the number of independent sources can not exceed the number of mixture signals. In our work, we deal with the case when $n = m$. Based on the previous statistical assumptions, the source signals could be estimated by [6]

$$\hat{\mathbf{s}}(k) = \mathbf{F}\mathbf{y}(k), \tag{2}$$

where $\mathbf{F}$ is an $m \times n$ separating matrix. Among the algorithms used to compute the separating matrix and the independent components, FastICA (a MATLAB package freely available [7]) is used here due to its fast convergence.

The FastICA algorithm is applied to the selected data. Once the independent components are computed, each one is fitted by an Autoregressive Moving-Average model of orders p and q (ARMA(p,q)). As in [5], the model order p for the autoregressive (AR) parameters is chosen as 4. The model order q for the Moving-Average (MA) parameters is chosen as $q = p - 1$. The ARMA parameters are estimated using Prony's method [8]. The AR parameters as well as the MA parameters are used to construct the matrices for the SSM. The SSM is expressed as [9]

$$\mathbf{s}(k) = \mathbf{A}\mathbf{s}(k-1) + \mathbf{B}\eta(k), \qquad \textit{(system model)} \tag{3}$$

$$\mathbf{y}(k) = \mathbf{C}\mathbf{s}(k) + \mathbf{D}\varepsilon(k), \qquad \textit{(observation model)} \tag{4}$$

where $\mathbf{s}(k)$ is an unobserved vector, referred to as the state; $\eta(k)$ is the white Gaussian system noise with zero mean and covariance matrix $\mathbf{Q}$; and $\varepsilon(k)$ is the white Gaussian observation noise with zero mean and covariance matrix $\mathbf{R}$. In ICA the observation noise is neglected; therefore, the second term of the observation model is removed. The states are estimated by means of a linear Kalman filter. These estimates are improved using the Rauch-Tung-Striebel (RTS) smoother.

For this IC-SSM, the coefficient matrices $\mathbf{A}$, $\mathbf{B}$ and $\mathbf{C}$ are time-invariant and the observation noise is zero [9]. Matrices $\mathbf{A}$ and $\mathbf{B}$ are formed using the observer canonical form. A detailed explanation of how the matrices $\mathbf{A}$, $\mathbf{B}$, $\mathbf{C}$ and $\mathbf{Q}$ are constructed is given in [3].

The obtained initial state-space model is optimized in the same manner as in [10], and in [5].

B. Augmentation of the State-Space Model and Suppression of Muscle Artifacts

The generated IC-SSM model, described so far, has at most n components containing brain activity only.

Since we aim at suppressing muscle artifacts, a different segment from the same electrodes, contaminated with muscle artifacts, is selected from the same data set. This segment does not need to be consecutive to the clean segment. Then, using the dynamical templates from step *A* as an initial model for the Kalman filter, the prediction errors or innovations (i.e., the differences between the actual and the estimated data) are computed. We expect that the muscle artifacts are contained within those prediction errors. The model is then augmented by extracting and adding components from the innovations representing the muscle artifacts. With this step, the case $n < m$ is obtained and the muscle artifacts are well separated from the brain activity.

The additional components contribute with further AR, MA and observation parameters which are all optimized according to maximum-likelihood; only those parameters of the new components are optimized, assuming that the brain dynamics are stationary.

If the additional components describe the artifacts having strong changes of variances during time, a stationary state-space model would not be appropriate. The Generalized Autoregressive Conditional Heteroscedasticity (GARCH) model is a way to introduce non-stationarity in a completely data-driven manner. In order to decide which component should be given to GARCH, we iteratively omit each component from this state-space model. The component, which produces the largest drop of the likelihood by being omitted, is selected for application of GARCH [10].

By applying GARCH, the state variances are better adapted to non-stationarities of the data; this improves the predictive performance of the model. The parameters of the added components, including those modeled with GARCH, are optimized as described above.

Once the model is optimized, the components identified as artifactual are completely removed, and the remaining components are transformed back to data space.

The distance between the power spectra of the artifacts-free segment and the segment with artifacts, before and after cleaning, as well as the distance between the power spectra of two segments without artifacts are computed to demonstrate the effectiveness of our approach. The distances have been calculated in a similar manner as in [11] as follows:

$$D = 10 \cdot \log \left(\frac{mean\left(\frac{Pow\_Segment\_One}{Pow\_Segment\_Two}\right)}{geomean\left(\frac{Pow\_Segment\_One}{Pow\_Segment\_Two}\right)} \right), \tag{5}$$

where *mean* refers to the arithmetic mean and *geomean* to the geometric mean. *Pow_Segment_One* and *Pow_Segment_Two* denote the power spectrum of the segments that are considered for computation. The closer to zero the distance is, the more similar the spectra are.

III. Application to Real Data

Real EEG data from an epilepsy patient are employed here to demonstrate the functionality of the algorithm discussed so far. For this study, we first choose a 20 s segment of 6 selected channels, exhibiting strong epileptic spikes and no

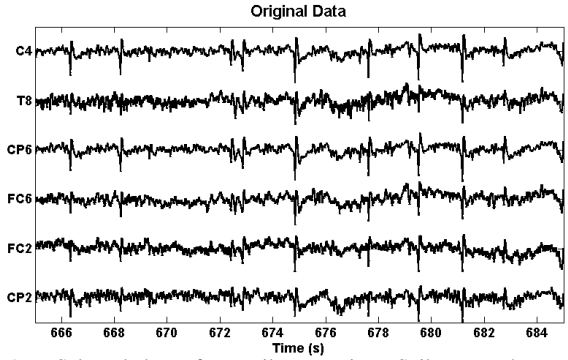

Fig. 1. Selected data of an epilepsy patient. Spikes are observed. No artifacts are present.

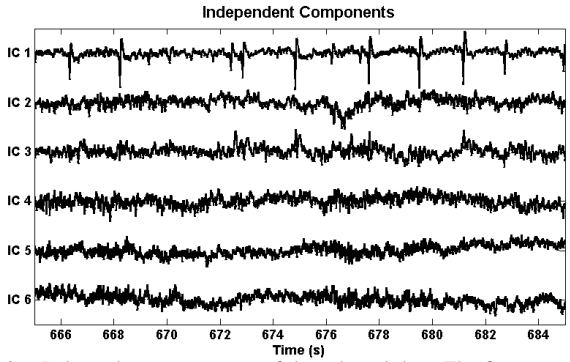

Fig. 2. Independent components of the selected data. The first component corresponds to the spikes.

artifacts. These data are used as a standard, which contains the expected brain signals without artifacts. Originally, the sampling frequency is 5000 Hz, but for practical reasons we have downsampled the data using a subsampling factor of 5 in order to reduce the sampling frequency to 1000 Hz. Fig. 1 shows the raw data; the epileptic spikes are clearly visible.

The independent components, obtained by FastICA, are presented in Fig. 2. The spikes can be observed mainly in the first component. As explained before, at most six components can be obtained with the FastICA algorithm.

Each independent component is fitted by an ARMA(4,3) model. The states are then estimated using a Kalman filter as described above and the SSM is optimized by maximum-likelihood. In Fig. 3, the filtered states after optimization are shown; it can be seen that the ICA components are still quite well reproduced, although they are in different order. At this point the model does not contain any artifacts.

In order to suppress the muscle artifacts, a 20 s segment contaminated with muscle artifacts is chosen, as shown in the

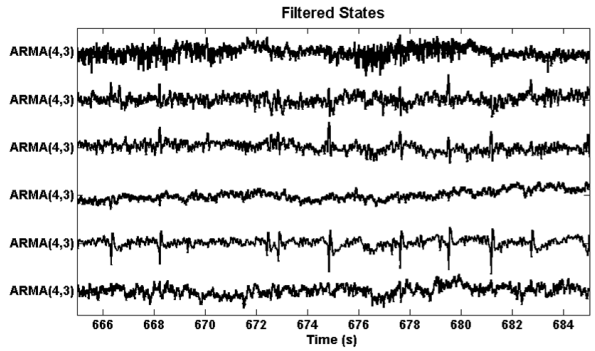

Fig. 3. Filtered states, after combining ICA-SSM and after optimization.

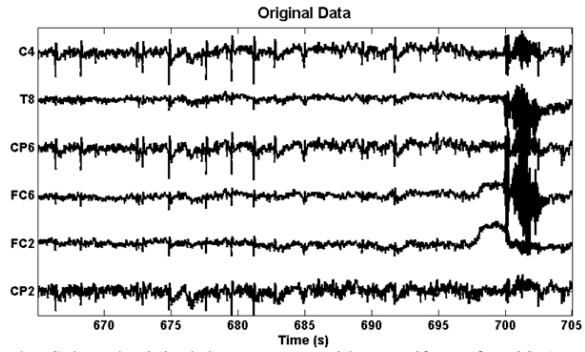

Fig. 4. Selected original data segment without artifacts (first 20 s) and the data segment contaminated with muscle artifacts (last 20 s).

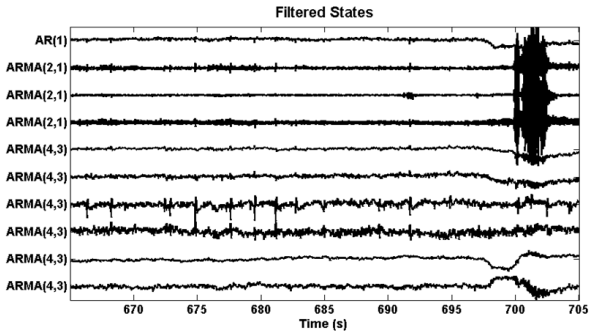

Fig. 5. Filtered states after augmenting the model, after applying GARCH to the third component and after optimization. The first four components correspond to the muscle artifacts. Fifth and tenth component contain some residual artifact, but in a negligible extent.

right half of Fig. 4. In this case, the segment without artifacts and the one contaminated with artifacts are consecutive. However, as mentioned before, this does not need to be the case. As observed in Fig. 4, the last 5 s exhibit the presence of strong muscle artifacts mainly in four electrode signals. Using the optimized model already constructed, and through applying a linear Kalman filter in an "out-of-sample" mode, the innovations are obtained. The model is then augmented by extracting and adding one AR(1) and three ARMA(2,1) components from the innovations. The number of components to be added is subjective. They are selected by visual inspection with the criterion that they should represent the muscle artifacts.

GARCH is applied to the most important artifact component and the augmented model is optimized, as described above. Only the four added components are optimized. Fig. 5 shows the augmented model after applying GARCH and after optimization. The four topmost curves represent the added components that contain muscle artifacts. As can be observed, the artifacts and the brain activity are well separated. Some residual muscle artifacts are still present in the fifth and the tenth component, counting from the top, but this contribution is very low compared to the one of the first four components.

The first four components are removed completely, and the final filtered data are obtained by transforming the remaining six components back to data space. The filtered signals are shown in Fig. 6. By visual inspection of this figure, the muscle artifacts are hardly observed, while brain activity (e.g. spikes) is still well preserved.

The distances between the power spectra of the segments

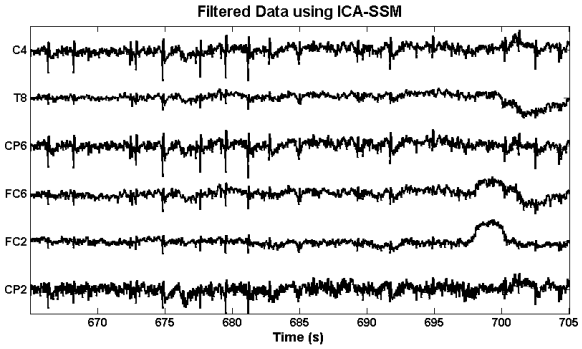

Fig. 6. Data of Fig. 4 after filtering. The muscle artifacts in the last 5 s are no longer visible.

with and without artifacts, before (D_{Art}) and after (D_{Filt}) cleaning, have been computed. We expect that after filtering both spectra are very similar. That is an indication that the artifacts have been suppressed. We have also computed the distance between the power spectra of two artifacts-free segments (D_{CC}). For this case, we expect that D_{Filt} and D_{CC} have similar values. That suggests that the filtered artifact segment and the segments without artifacts contain just brain activity. Table I shows the results.

TABLE I

DISTANCE COMPARISON BEFORE (D_{Art}) AND AFTER (D_{Filt}) FILTERING, AND CONSIDERING TWO ARTIFACTS-FREE SEGMENTS (D_{CC})

Electrode	D_{Art}	D_{Filt}	D_{CC}
C4	10.94	0.78	0.44
T8	12.01	1.23	0.95
CP6	10.69	0.70	0.34
FC6	13.71	0.40	0.71
FC2	4.52	1.23	0.58
CP2	4.72	1.83	0.46

As observed in Table I, the distances are considerably reduced after cleaning. The values of D_{Filt} are about the same size as the values of D_{CC}, indicating that the filtered segment is similar to the artifacts-free segments. Consequently the muscle artifacts must have been reduced to a large extent.

IV. CONCLUSIONS

In this paper the suppression of muscle artifacts by means of the combination of an instantaneous ICA algorithm and SSM is presented. The suppression of muscle artifacts has been achieved by constructing first an initial model for data without artifacts from the results of ICA. Then, a segment with muscle artifacts is chosen. Using the initial model and through the Kalman filter the innovations are computed, which mainly describe the muscle artifacts. The state-space is augmented by extracting additional artifactual components from the innovations, which correspond to the muscle artifacts to be removed afterwards.

It has been shown that GARCH models can be applied to one (or more) of the components that represent the muscle artifacts, due to their non-stationary behavior, thereby improving the quality of the model.

The filtered signals have been obtained by removing the components that contain the muscle artifacts and then transforming the other components back to data space.

Compared to the pure ICA algorithms, the combined ICA-SSM algorithm overcomes the constraint of ICA of having at most the same number of components as channels. In other words, the case of $n < m$ is achieved. This leads to a proper separation of muscle artifacts from brain information. Therefore, as has been graphically shown, the proposed algorithm suppresses to a large extent the muscle artifacts, while preserving the brain activity.

Using the distance between the power spectra as an indicator, we have demonstrated quantitatively that our algorithm has succeeded in reducing muscle artifacts. After filtering, the distance is closer to zero and it differs by an small amount to the distance between the power spectra of the artifacts-free segments. That suggests that the muscle artifacts have been considerably and efficiently reduced. However, we note that for most channels D_{Filt} is slightly larger than D_{CC}. That might happen because of two reasons: either there is a weakness in the spectral estimate of the filtered segment, or there are some residual muscle artifacts that our approach has not discriminated. Further research will address this issue.

The selection of the muscle artifacts segments, as well as the selection of the artifactual components to be removed, have been done by visual inspection. Further research will focus on its automatic identification and suppression, as well as on the suppression of other kind of artifacts such as scanner (fMRI) artifacts.

ACKNOWLEDGMENT

The authors would like to thank the German Research Foundation (Deutsche Forschungsgemeinschaft, DFG) who funded this work through the Collaborative Research Center SFB 855 "Biomagnetic Sensing".

REFERENCES

[1] S. Sanei and J. A. Chambers, *EEG Signal Processing*. England: John Wiley and Sons, Ltd, 2007, pp. 14-20

[2] W. De Clercq, A. Vergult, B. Vanrumste, W. Van Paesschen, and S. Van Huffel, "Canonical correlation analysis to remove muscle artifacts from the electroencephalogram". *IEEE Trans. on Biomedical Engineering*, pp. 2583-2587, 2006.

[3] A. Galka, K. F. K. Wong, T. Ozaki, H. Muhle, U. Stephani and Michael Siniatchkin, "Decomposition of neurological multivariate time series by state space modelling", *Bulletin of Mathematical Biology*, vol. 73, pp. 285-324, 2011.

[4] H. Nam, T.-G. Yim, S. K. Han, J.-B Oh, and S. K. Lee, "Independent component analysis of ictal EEG in medial temporal lobe epilepsy". *Epilepsia*, vol. 43, pp. 160-164, 2002.

[5] A. Santillán-Guzmán, A. Galka, U. Heute, and U. Stephani, "Application of state-space modeling to instantaneous independent-component analysis", in *Proc. 4th International Conference on Biomedical Engineering and Informatics*, Shanghai, 2011, pp. 643-646.

[6] R. Vigário, J. Särelä, V. Jousmäki, M. Hämäläinen and E. Oja, "Independent component approach to the analysis of EEG and MEG recordings", *IEEE Trans. on Biomedical Engineering*, vol. 47, pp. 589-593, May 2005.

[7] FastICA MATLAB Package [Online]. Last accessed: Nov. 2010. http://www.cis.hut.fi/projects/ica/fastica.

[8] D. L. Jones, "Prony's method" [Online]. Last accessed: Apr. 2011. http://cnx.org/content/m12762/1.2/.

[9] G. Kitagawa, *Introduction to Time Series Modeling*, Taylor and Francis Group, LLC, 2010, pp. 135-138, 151-153 and 203-204.

[10] A. Galka, K. F. K. Wong and T. Ozaki, "Generalized state space models for modelling non-stationary EEG time series" in *Modelling phase transition in the brain. Springer Series in Computational Neuroscience*, A. Steyn-Ross, M.Steyn-Ross, Eds., New York: Springer, Berlin, Heidelberg, 2010, pp. 27-52.

[11] T. T. Georgiou, "Distances between power spectral densities", *IEEE Trans. on Signal Processing*, vol. 55, pp. 3995-4003, August 2007.